

# A Data-Driven Aggressive Autonomous Racing Framework Utilizing Local Trajectory Planning with Velocity Prediction

Zhouheng Li<sup>1</sup>, Bei Zhou<sup>1</sup>, Cheng Hu<sup>1</sup>, Lei Xie<sup>1,†</sup>, Hongye Su<sup>1</sup>

**Abstract**—The development of autonomous driving has boosted the research on autonomous racing. However, existing local trajectory planning methods have difficulty planning trajectories with optimal velocity profiles at racetracks with sharp corners, thus weakening the performance of autonomous racing. To address this problem, we propose a local trajectory planning method that integrates Velocity Prediction based on Model Predictive Contour Control (VPMPCC). The optimal parameters of VPMPCC are learned through Bayesian Optimization (BO) based on a proposed novel Objective Function adapted to Racing (OFR). Specifically, VPMPCC achieves velocity prediction by encoding the racetrack as a reference velocity profile and incorporating it into the optimization problem. This method optimizes the velocity profile of local trajectories, especially at corners with significant curvature. The proposed OFR balances racing performance with vehicle safety, ensuring safe and efficient BO training. In the simulation, the number of training iterations for OFR-based BO is reduced by 42.86% compared to the state-of-the-art method. The optimal simulation-trained parameters are then applied to a real-world F1TENTH vehicle without retraining. During prolonged racing on a custom-built racetrack featuring significant sharp corners, the mean velocity of VPMPCC reaches 93.18% of the vehicle’s handling limits. The released code is available at <https://github.com/zhouhengli/VPMPCC>.

## I. INTRODUCTION

Autonomous racing stems from the development of autonomous driving. Pushing vehicle performance to its limits is the goal of autonomous racing. This poses a significant challenge to local trajectory planning methods due to the following four factors: (a) minimum lap time guarantee [1]–[3]; (b) control feasibility of the planned trajectory [4], [5]; (c) computational efficiency of the optimization problem [6], [7]; and (d) safe and efficient parameters tuning [8]–[10]. Global trajectory planning [1], [11] leverages complete racetrack information for racing trajectory planning. However, it fails to account for real-time vehicle state changes, causing control issues and thus reducing racing performance. Recently, local trajectory planning methods integrating planning and control have been widely studied [12]–[15]. Model Predictive Contour Control (MPCC) is a typical example of such an approach [13], [14]. To realize minimum lap time, MPCC introduces the projected velocity as an effective metric to represent the racing progress. This method performs well on racetracks without significant curvature corners [14].

This work was supported by the Ningbo Key research and development Plan (No.2023Z116).

<sup>†</sup> Corresponding author.

<sup>1</sup>Zhouheng Li, Bei Zhou, Cheng Hu, Lei Xie, and Hongye Su are with the State Key Laboratory of Industrial, Zhejiang University, Hangzhou 310027, China. {zh.li, zhoubei, 22032081}@zju.edu.cn; {leix, hysu}@iipc.zju.edu.cn.

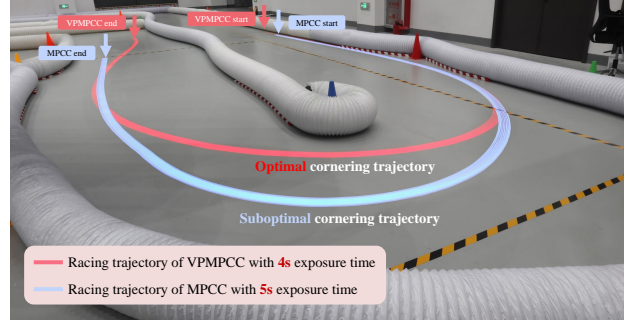


Fig. 1. Comparison of trajectories between the proposed Velocity Prediction MPCC (VPMPCC) and standard MPCC through a high-curvature corner using a self-built F1TENTH vehicle. The trajectories are captured through long exposures. VPMPCC is able to plan optimal cornering trajectories at higher velocities, resulting in shorter cornering time to reduce lap time.

However, with sharp corners on the racetrack (as shown in Fig. 1), relying solely on tracking error to balance the projected velocity maximization makes it difficult for MPCC to plan cornering trajectories with optimal velocities [16]. To tackle this problem, we propose a Velocity Prediction MPCC (VPMPCC) local trajectory planning method. Specifically, the proposed VPMPCC realizes velocity prediction by using vehicle longitudinal velocity as an independent velocity decision variable. The key advantage lies in optimizing the velocity profile of the local trajectory, particularly on corners with significant curvature, ultimately reducing lap time.

In recent years, data-driven Bayesian optimization (BO) [8], [9], [17] has been developed to realize automatic parameters tuning. However, these methods do not consider modeling vehicle safety while reducing lap time, resulting in the inability to guarantee vehicle safety during generalization [18]. Meanwhile, simultaneously ensuring the accuracy of the vehicle model and achieving computational efficiency of the optimization problem is also a primary challenge [5], [6]. To bridge these gaps, a safe and efficient data-driven racing framework is proposed, incorporating the VPMPCC and BO. Specifically, in closed-loop BO training, the proposed framework uses the high-fidelity vehicle dynamics model obtained from offline system identification to filter the racing trajectory planned by the vehicle kinematic model-based VPMPCC. Moreover, a practical Objective Function adapted to Racing (OFR) is designed for BO to achieve efficient training. The advantage of this framework is that the parameters of the VPMPCC planner can be safely trained in the simulation and transferred to real-world vehicles without

retraining. Therefore, the vehicle performance can be pushed to its limits efficiently and safely. In summary, this paper provides the following contributions:

- 1) **An effective method for integrating velocity prediction to efficiently optimize local trajectory velocity profiles.** The proposed VPMPC integrates velocity prediction into trajectory planning by encoding the racetrack as a Reference Velocity Profile (RVP). Velocity prediction is then achieved by matching the planned velocities within the prediction horizon with the corresponding reference velocities in the RVP.
- 2) **An effective OFR accelerates BO to safely learn the optimal parameters of the local trajectory planner.** The proposed OFR enhances vehicle safety by limiting racing trajectory deviations significantly from the reference line and reduces the number of iterations required for convergence by applying negative costs to time-reducing trajectories. It improves training efficiency by **42.86%**, with optimal simulation parameters transferable to real-world vehicles.
- 3) **A data-driven autonomous racing framework safely pushes the vehicle to its handling limits, validated through well-established and reliable real-world vehicle experiments.** The VPMPC and BO-based autonomous racing framework (VPBO-RF) demonstrates superior performance on a self-built 1:10 scale F1TENTH vehicle, excelling on a challenging race-track with several sharp corners. Despite limited computational resources and execution delays, the mean velocity of VPMPC achieved **93.18%** of vehicle handling limits, with an efficient mean computation time of **7.04 ms**.

This paper consists of several sections. Section II introduces MPCC and the system dynamic of VPMPC, followed by an overview of BO. Section III introduces the implementation of VPMPC. Section IV describes the overall framework of VPBO-RF, focusing on the design of the OFR. Section V includes simulations and real-world experiments, while Section VI serves as the conclusion, summarizing the essential findings and outlining directions for future research.

## II. PRELIMINARIES

This section includes an introduction to MPCC and the system dynamics of VPMPC, followed by an overview of conventional BO.

### A. Model Predictive Contouring Control

As shown in Fig. 2, the contour error  $e_{\text{con}}$  and the lag error  $e_{\text{lag}}$  of MPCC [13] are calculated as follows:

$$\begin{aligned} e_{\text{con},s} &= \mathbf{n}_s \cdot (\mathbf{p} - \boldsymbol{\tau}_s), \quad e_{\text{lag},s} = \mathbf{t}_s \cdot (\mathbf{p} - \boldsymbol{\tau}_s) \\ \mathbf{e}_s &= [e_{\text{con},s} \quad e_{\text{lag},s}]^\top, \quad \mathbf{c} = [(e_{\text{con}}^{\text{max}})^{-1} \quad (e_{\text{lag}}^{\text{max}})^{-1}] \end{aligned} \quad (1)$$

where  $\mathbf{p} = [x \quad y]^\top$  represents the position of the rear axle center in the Cartesian frame. The reference line, denoted by  $\boldsymbol{\tau}$ , is parameterized by the arc length  $s$ . For a given arc length  $s$ ,  $\mathbf{n}_s$  and  $\mathbf{t}_s$  are the normal and tangent unit vectors of the

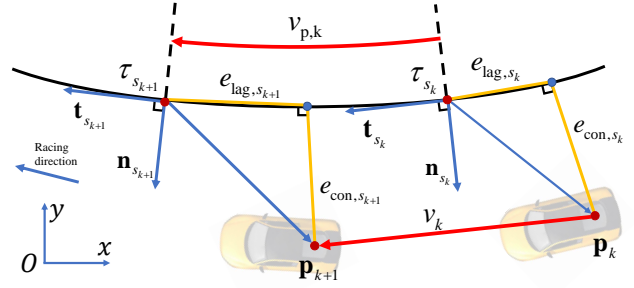


Fig. 2. Schematic diagram illustrating the calculation of contour and lag errors in conventional MPCC. The proposed VPMPC method incorporates the vehicle's longitudinal velocity as an independent decision variable.

reference point  $\boldsymbol{\tau}_s = [x_{\boldsymbol{\tau},s}, y_{\boldsymbol{\tau},s}]$ . And  $\mathbf{c}$  is the normalization vector for the tracking error  $\mathbf{e}_s$ . The MPCC approximates the projected velocity  $v_p$  to the vehicle longitudinal velocity  $v$ , expressed as  $v_p \approx v$ . Then, with the help of  $\mathbf{e}_s$  and  $v_p$ , the composition of the cost function of MPCC is shown below:

$$f_{\text{MPCC}} = - \sum_{k=1}^{N_p} \frac{\gamma \cdot v_{p,k}}{v_{\text{max}}} + \|\mathbf{c} \cdot \mathbf{e}_{s_k}\|_{\mathbf{q}_e}^2 + \|\mathbf{u}_{k+1} - \mathbf{u}_k\|_{\mathbf{R}}^2 \quad (2)$$

where  $N_p$  denotes the prediction horizon and  $\gamma$  is the scalar weight of maximum projected velocity. The weight matrix  $\mathbf{q}_e$  for contour and lag errors is  $\text{diag}([q_{e_{\text{con}}} \quad q_{e_{\text{lag}}}]$ , and the weight matrix  $\mathbf{R}$  is for the change of control variables.  $v_{\text{max}}$  is the maximum longitudinal velocity used for normalization.

### B. System Dynamics

In contrast to the conventional MPCC, VPMPC decouples the projected velocity  $v_p$  from the vehicle longitudinal velocity  $v$ . The advantage of this design is that the introduction of velocity prediction can be a trade-off with maximizing the projected velocity at corners with significant curvature. Therefore, the system dynamics used by VPMPC is:

$$\begin{aligned} \dot{x} &= \cos(\varphi) \cdot v \\ \dot{y} &= \sin(\varphi) \cdot v \\ \dot{\varphi} &= v \cdot \tan(\delta) \cdot L^{-1} \\ \dot{s} &= v_p \end{aligned} \quad (3)$$

where  $\varphi$  is the yaw angle and  $L$  is the wheelbase. Then let  $\boldsymbol{\zeta} = [x, y, \varphi, s]^\top$  denotes the state space, and  $\mathbf{u} = [v, \delta, v_p]^\top$  denotes the configuration space. The final control inputs for the underlying chassis are  $v$  and steering angle  $\delta$ . Therefore, the weight matrix  $\mathbf{R}$  in (2) is expressed as  $\text{diag}([q_{\Delta v} \quad q_{\Delta \delta} \quad q_{\Delta v_p}])$ .

### C. Bayesian Optimization

The BO aims to solve the following optimization problem given a series of observations  $\mathbf{z}$ :

$$\boldsymbol{\theta}^* = \arg \min_{\boldsymbol{\theta} \in \Theta} J(\boldsymbol{\theta}; \mathbf{z}) \quad (4)$$

where  $J_{\boldsymbol{\theta}}$  denotes the objective function, which a surrogate model approximates.  $\boldsymbol{\theta}$  is the optimization variable. And  $\Theta$  denotes the feasible space of all optimization parameters.

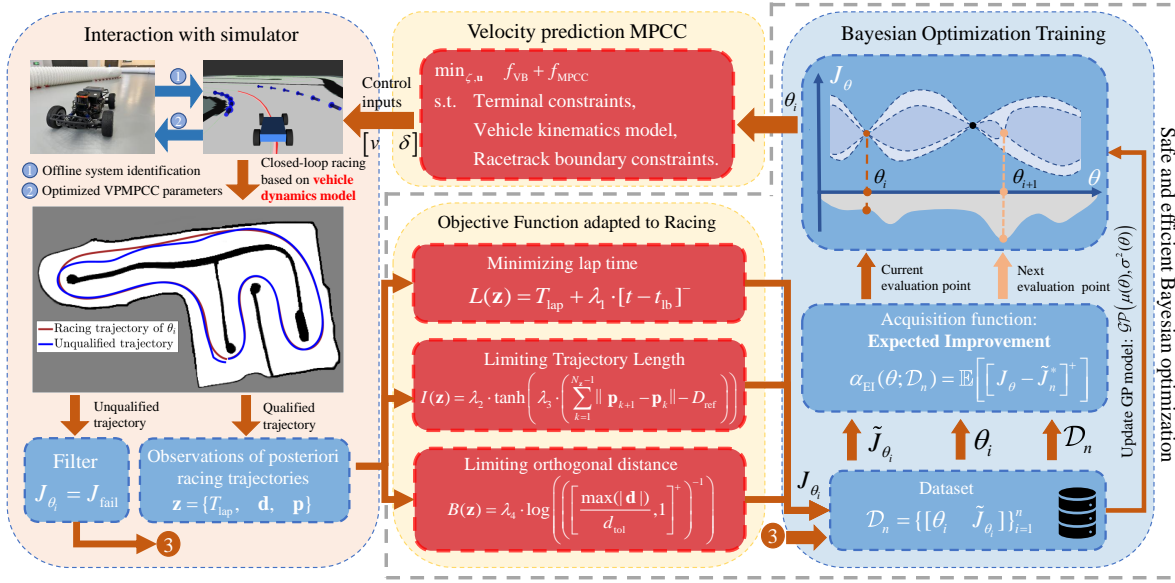


Fig. 3. Schematic diagram of the VPBO-RF. The **brown** arrows indicate the online evaluation process of parameter  $\theta_i$ . The **light brown** arrows indicate the next evaluation parameter  $\theta_{i+1}$  chosen by the acquisition function. The closed-loop training convergence means that the OFR value no longer decreases.

The Gaussian Process (GP) is the most widely used surrogate model denoted as  $J_\theta \sim \mathcal{GP}(\mu(\theta), \sigma^2(\theta))$ ,  $\mu(\theta)$  is the mean function, and  $\sigma^2(\theta) = \mathcal{K}(\theta_i, \theta_j)$  is the kernel function. To initialize the GP model, full-space random sampling is performed within the feasible space  $\Theta$  to construct the priori dataset, which is denoted as  $\mathcal{D}_n = \{[\theta_i, \tilde{J}_{\theta_i}]\}_{i=1}^n$ , where  $n$  is the number of random samples and  $\tilde{J}_{\theta_i} = J_{\theta_i} + \eta$ . Here,  $\eta$  is the Gaussian-distributed noise with mean 0 and covariance  $\sigma_\eta$ . During the prediction of the selected evaluation point  $\theta_i$ , the dataset  $\mathcal{D}_n$  is utilized to construct the covariance matrix  $\mathbf{K}_n = [\mathcal{K}(\theta_i, \theta_j)]_{i,j=1}^n$  and covariance vector  $\mathbf{k}_n = [\mathcal{K}(\theta^*, \theta_i)]_{i=1}^n$ . Then, the selected evaluation points are determined using the acquisition function [19].

### III. VELOCITY PREDICTION MPCC

This section outlines the implementation of VPMPPC, emphasizing velocity prediction, and discusses the trade-off between velocity prediction and maximizing projected velocity.

#### A. Design of the Velocity Prediction

The VPMPPC is proposed to optimize the velocity profile for local trajectory planning on racetracks with sharp curvature corners. The velocity prediction is accomplished by enhancing the similarity between planned velocities in the prediction horizon and the corresponding reference velocity in RVP, which is parameterized by the arc length as  $v_{RVP,s}$ . Therefore, the following objective function for velocity prediction can be constructed:

$$f_{VP} = \frac{q_v}{v_{\max}} \sum_{k=1}^{N_p} (v_k - v_{RVP,s_k})^2 \quad (5)$$

where  $v_{\Delta, \max}$  denotes the maximum error in velocity matching. The  $q_v$  is a scalar weight. VPMPPC uses the minimum curvature path of [11] as the reference line and the

corresponding velocity profile as the RVP. The VPMPPC controls the racing performance through the velocity prediction component  $f_{VP}$  and the maximizing projected velocity component in the (2) together. At racetrack corners with high curvature, maximizing the projected velocity component incurs a significant cost in the velocity prediction component. This forces the optimization problem to shift from the aggressive decision of maximizing the vehicle's projected velocity to the safer decision of reducing the velocity. It is important to note that the RVP is used only for velocity prediction, not velocity tracking. This distinction is the fundamental difference between VPMPPC and longitudinal velocity tracking controllers [20].

#### B. VPMPPC Formation

According to (5) and (2), the final VPMPPC optimization problem can be summarized as:

$$\begin{aligned} \min_{\zeta, \mathbf{u}} \quad & f_{VP} + f_{MPCC} \\ \text{s.t.} \quad & \zeta_{k+1} = \zeta_k + T_s \cdot f(\zeta_k, \mathbf{u}_k), \zeta_0 = \zeta_{\text{cur}}, \\ & \zeta_{\min} \leq |\zeta_k| \leq \zeta_{\max}, \mathbf{u}_{\min} \leq |\mathbf{u}_k| \leq \mathbf{u}_{\max}. \end{aligned} \quad (6)$$

where  $\zeta_{\max}$  and  $\zeta_{\min}$  denote the upper and lower bounds of the state constraints, while  $\mathbf{u}_{\max}$  and  $\mathbf{u}_{\min}$  are the upper and lower limits of the control variable, respectively.  $T_s$  is the prediction interval, and  $\zeta_{\text{cur}}$  is current state values. The racetrack width is scaled using  $\kappa < 1$ , ensuring the planned trajectory remains fully within the racetrack for safety.

### IV. DATA-DRIVEN AUTONOMOUS RACING FRAMEWORK UTILIZING HIGH-EFFICIENCY OFR-DRIVEN BO

This section outlines the OFR design, focusing on racing performance and vehicle safety modeling, followed by the method for filtering abnormal trajectories using the vehicle dynamics model. The overall training framework is shown in

Fig. 3. The vehicle dynamics model used during BO training and the system identification method are detailed in [21]. The parameters of the proposed VPMPCC to be optimized are expressed in the following form:

$$\boldsymbol{\theta} = [N_p \quad q_v \quad \gamma \quad e_{\text{con}} \quad e_{\text{lag}} \quad q_{\Delta v} \quad q_{\Delta \delta} \quad q_{\Delta v_p} \quad \kappa]_{9 \times 1}^\top$$

where the meaning of the parameters in  $\boldsymbol{\theta}$  is described in detail in Section II and III. The observations chosen for BO is  $\mathbf{z} = \{T_{\text{lap}}, \mathbf{d}, \mathbf{P}\}$ .  $T_{\text{lap}}$  denotes lap time.  $\mathbf{d} = [d_1, \dots, d_{N_z}]$  is the orthogonal distance of the racing trajectory corresponding to the reference line.  $\mathbf{P} = [\mathbf{p}_1, \dots, \mathbf{p}_{N_z}]$  is the list of the racing trajectory points.  $N_z$  is the number of trajectory points. The number of training episodes is  $N_{\text{BO}}$ .

1) *Surrogate model*: The OFR denoted as  $J_\theta$  consists of the following components: lap time, trajectory length minimization, and limitations on orthogonal distance. Firstly, the modeling of  $L(\mathbf{z})$  encourages VPMPCC to explore lower lap time is:

$$L(\mathbf{z}) = T_{\text{lap}} + \lambda_1 \cdot [t - t_{\text{lb}}]^- \quad (7)$$

where  $[a]^- = \min(a, 0)$ , and  $t_{\text{lb}}$  denotes the threshold for reducing objective function value.

Then, the trajectory length minimization is modeled as:

$$I(\mathbf{z}) = \lambda_2 \cdot \tanh \left( \lambda_3 \cdot \left( \sum_{i=1}^{N_z-1} \|\mathbf{p}_{i+1} - \mathbf{p}_i\| - D_{\text{ref}} \right) \right) \quad (8)$$

where  $\lambda_2, \lambda_3$  achieves a trade-off between different components.  $D_{\text{ref}}$  is the length of the reference line. The purpose of this component is to force VPMPCC to search for shorter racing trajectories, thereby accelerating the exploration of minimal lap time.

The limitation on the orthogonal distance of racing trajectory using the log barrier function is presented below:

$$B(\mathbf{z}) = \lambda_4 \cdot \log \left( \left( \left[ \frac{\max(|\mathbf{d}|)}{d_{\text{tol}}}, 1 \right]^+ \right)^{-1} \right) \quad (9)$$

where  $[a, 1]^+ = \max(a, 1)$ ,  $\lambda_4 < 0$ , and the  $d_{\text{tol}}$  denotes the maximum orthogonal distance at which the vehicle is allowed to deviate from the reference line. Normally,  $B(\mathbf{z})$  does not work, but it gives a large penalty when the vehicle deviates significantly. So the value of  $|\lambda_4|$  needs to be large.

The vehicle kinematics model cannot fully capture the dynamics of the vehicle, leading to abnormal trajectories during racing, as shown in Fig. 3. This is because control inputs calculated based on the vehicle kinematics model may lead to abnormal position shifts after being integrated over time by the vehicle dynamics model. During BO training, these abnormal trajectories are identified as unqualified and penalized through  $J_{\text{fail}}$ , preventing BO from further exploring the unqualified trajectories generated by the kinematic model. Therefore, the  $J_\theta$  can be expressed as:

$$J_\theta = \begin{cases} J_{\text{fail}}, & \text{if } \Delta \mathbf{p} \geq d_{\text{ub}} \text{ or } D_{\text{traj}} < D_{\text{lb}}, \\ L(\mathbf{z}) + I(\mathbf{z}) + B(\mathbf{z}), & \text{otherwise.} \end{cases} \quad (10)$$

where  $\Delta \mathbf{p} = \|\mathbf{p}_i - \mathbf{p}_{i+1}\|, \forall i \in [1, \dots, N_z-1]$ . The  $d_{\text{ub}}$  denotes the maximum distance between neighboring points on the racing trajectory, and  $D_{\text{lb}}$  denotes the minimum racing trajectory length. The value of OFR for crashed and collision racing trajectories are all  $J_{\text{fail}}$ .

2) *Acquisition function*: The acquisition function chosen is expected improvement [22], which is represented as:

$$\alpha_{\text{EI}}(\boldsymbol{\theta}; \mathcal{D}_n) = \mathbb{E} \left[ \left[ J_\theta - \tilde{J}_n^* \right]^+ \right] \quad (11)$$

where  $[a]^+ = \max(a, 0)$ . And  $\tilde{J}_n^*$  is best value to date. The next evaluation point  $\boldsymbol{\theta}_{i+1}$  is then selected using  $\boldsymbol{\theta}_{i+1} = \arg \max_{\boldsymbol{\theta} \in \Theta} \alpha_{\text{EI}}(\boldsymbol{\theta}; \mathcal{D}_n)$ . VPMPCC is then reconstructed based on  $\boldsymbol{\theta}_{i+1}$  for collecting new observations  $\mathbf{z}_{i+1}$ , which is used to enrich  $\mathcal{D}_n$ , thus completing the closed-loop training.

## V. EXPERIMENTAL RESULTS AND DISCUSSION

In this section, the superiority of the proposed VPBO-RF is validated through simulations and real-world experiments. The focus is on BO training efficiency in simulations and the vehicle's mean velocity, lap time (L.T), and computation time (C.T) during real-world racing using a self-built 1:10 scale F1TENTH vehicle (see Fig. 4a). A complex racetrack with four significant curvature corners (as shown in Fig. 4b) is built for simulation and real-world racing. The Cartographer ROS [23] is used for mapping and localization (see Fig. 4c).

### A. Effectiveness of the proposed OFR

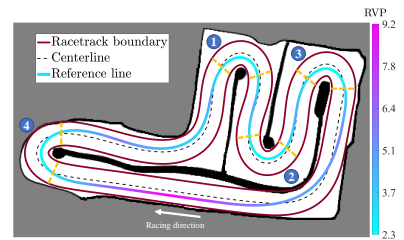
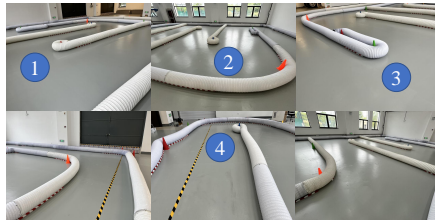
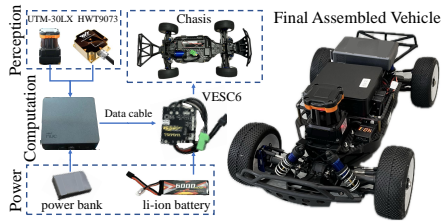
The runtime environment for the simulation and the F1TENTH vehicle is ROS Melodic on Ubuntu 18.04. BO training is implemented using the 'bayesopt' in Matlab. The CasADi [24] serves as the solver for the optimization problem of VPMPCC. The algorithm parameters related to VPBO-RF are shown in Table I. The comparison and ablation experiments constructed in the simulation are shown below:

- 1) Baseline (BL) [8]: The objective function is  $J_\theta = T_{\text{lap}} + \alpha \cdot \text{mean}(\mathbf{d})$ . Because the values of  $\mathbf{d}$  are small, the weight  $\alpha$  is used as a trade-off with the lap time;
- 2) Proposed OFR: The objective function is  $J_{\text{qualified}, \theta} = L(\mathbf{z}) + I(\mathbf{z}) + B(\mathbf{z})$ ;
- 3) Ablation1: The **trajectory length** is removed from the objective function:  $J_{\text{qualified}, \theta} = L(\mathbf{z}) + B(\mathbf{z})$ ;
- 4) Ablation2: The **lap time reduction** is removed from the objective function:  $J_{\text{qualified}, \theta} = T_{\text{lap}} + B(\mathbf{z}) + I(\mathbf{z})$ ;
- 5) Ablation3: The **orthogonal distance** is removed from the objective function:  $J_{\text{qualified}, \theta} = L(\mathbf{z}) + I(\mathbf{z})$ .

TABLE I

MAIN PARAMETERS OF THE PROPOSED VPMPCC AND BO-BASED AUTONOMOUS RACING FRAMEWORK.

Parameters	Setting	Parameters	Setting
$[N_{\text{BO}}, v_{\Delta, \text{max}}]$	[200, 10m/s]	$\lambda$	[20, 10, 0.5, -100]
$[L, T_s]$	[0.32m, 0.1s]	$\mathbf{u}_{\text{min}}$	[-15m/s -0.4rad -15m/s]
$[d_{\text{tol}}, t_{\text{lb}}]$	[0.5m, 17.6s]	$\mathbf{u}_{\text{max}}$	[15m/s 0.4rad 15m/s]
$[d_{\text{ub}}, D_{\text{ub}}]$	[0.6m, 60m]	$[e_{\text{con}}^{\text{max}}, e_{\text{lag}}^{\text{max}}]$	[0.5m 0.5m]

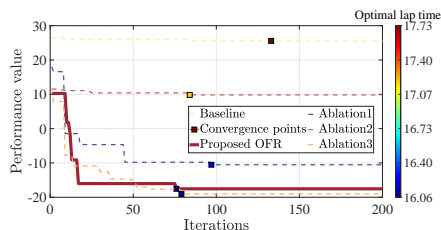


(a) Hardware of the self-built F1TENTH vehicle

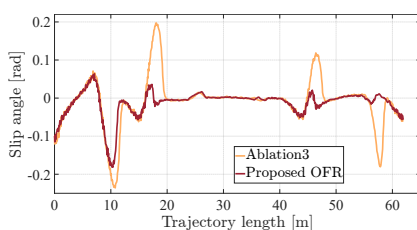
(b) Racetrack includes four sharp corners

(c) Grid map of the racetrack

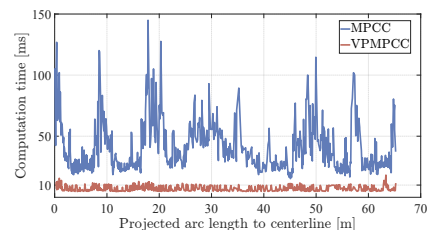
Fig. 4. The grid map created from real racetracks determines boundaries for VPMPC and is used for localization during real vehicle racing.



(a) BO training process



(b) Slip angles for racing trajectories



(c) Comparison of computation efficiency

Fig. 5. The different colored boxes ■ represent the optimal lap time obtained from training in Fig. 5a. The proposed Objective Function adapted to Racing enables BO to converge rapidly, and its optimal lap time outperforms the baseline. Ablation experiments demonstrate the effectiveness of different components of OFR for improving the training efficiency and safety of optimal trajectories.

TABLE II

STATISTICS FOR VERIFYING THAT THE PROPOSED OBF CAN IMPROVE THE BO TRAINING EFFICIENCY AND OPTIMAL LAP TIME

Type	Optimal lap time ↓	Comparison	Convergence iteration ↓	Comparison
BL [8]	17.73	-	133	-
Proposed	16.12	-9.07%	<b>76</b>	<b>42.86%</b>
Ablation1	16.26	-8.30%	97	27.07%
Ablation2	17.18	-3.09%	84	36.84%
Ablation3	<b>16.06</b>	<b>-9.40%</b>	79	40.60%

The training efficiency is calculated as  $\frac{N_{BL} - N_{opt}}{N_{BL}}$ , where  $N_{opt}$  is iterations required for BO convergence of different experiments. The percentage of racing performance improvement is calculated as  $\frac{T_{lap,BL} - T_{lap,opt}}{T_{lap,BL}}$ , where  $T_{lap,opt}$  is the optimal lap time. The lower bound of  $\theta$  is [5, 1, 1, 1, 1, 0.1, 1, 1, 0.01], and the upper bound is [60, 50, 10, 10, 10, 20, 50, 20, 0.4]. The  $D_{ref}$  is 62.8m and  $J_{inf}$  is 17.6. The results of BO learning based on different objective functions are shown in Fig. 5a and Table II. Compared with baseline, OFR significantly improves the training efficiency of BO by **42.86%**. In addition, the OFR converged lap time is also superior to baseline with a reduction of **9.07%**. Ablation1 and Ablation2 show lower training efficiency and less reduction in optimal lap time than the proposed OFR. This demonstrates the effectiveness of the trajectory length minimization and lap time reduction components of the proposed OFR. The training efficiency of Ablation3 is comparable to that of the proposed OFR, and it achieves a shorter lap time. However, the slip angle of the optimal trajectory from Ablation3 is significantly larger than that obtained through OFR-based training (as shown in

Fig. 5b). This suggests that limiting the maximum orthogonal distance of the racing trajectory can reduce slip angle. This is because OFR penalizes BO for exploring racing trajectories that deviate significantly from the reference line during training.

### B. Effectiveness of the proposed VPMPC

The MPCC proposed in [14] and the Velocity-Tracking Adaptive Pure Pursuit (VTAPP) controller proposed in [20] are used for comparison. The optimal parameters of MPCC are also trained through OFR-based BO, which is [13, 0, 39.0, 5.8, 0.6, 2.8, 0.2, 0.5, 0.02]. And MPCC uses the racetrack centerline as the reference line. The optimal parameters of VPMPC trained by BO based on the proposed OFR is  $\theta^* = [6, 3, 6, 3.9, 1, 19.0, 28, 15.7, 0.3]$ . These three methods are used to perform consecutive laps of racing to verify the superiority of the VPMPC method in terms of high performance and stability. The statistical data is shown in Table III.

The mean velocity of VPMPC reaches **93.18%** of vehicle handling limits, much higher than the other methods. It also has a low computation time of **7.04ms**, which indicates that VPMPC has high real-time performance. VPMPC has consistently raced for **25** laps at a maximum velocity of **6.39 m/s**, demonstrating its stability. This successfully proves that VPMPC pushes the vehicle performance to its limits with stability. Compared to VTAPP, VPMPC maintains the effect of maximum projected velocity, thus planning local trajectories with superior velocities, especially in corners (as shown in Fig. 6a). As shown in Fig. 6b, during a single lap, the racing velocities of VPMPC are significantly higher than those of MPCC. This is because MPCC employs an

TABLE III

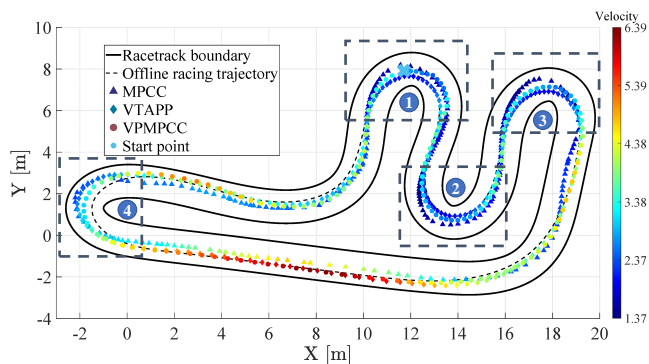
THE STATISTICS OF CONTINUOUS AUTONOMOUS RACING TRAJECTORIES VALIDATE THAT VPMPPC PUSHES VEHICLE PERFORMANCE TO ITS LIMITS WHILE MAINTAINING STABILITY ON A CHALLENGING RACETRACK WITH FOUR SHARP CORNERS.

Methods <sup>1</sup>	Mean(L.T)	Compare <sup>2</sup> ↓	Mean( $v$ )	Compare <sup>3</sup> ↑	Max( $v$ )	Laps	Std(C.T)	Mean(C.T)	Std(Cost)	Std( $a_x$ )
vehicle limits [11]	15.88s	-	3.95 m/s	-	9.16m/s	-	-	-	-	-
MPCC [14]	30.44s	47.82%	2.15 m/s	54.41%	4.91m/s	7	19.52	36.37ms	6.16	0.65m/s <sup>2</sup>
VTAPP [20]	19.90s	20.18%	3.16 m/s	79.82%	6.25m/s	25	-	-	-	1.03m/s <sup>2</sup>
VPMPPC-proposed	<b>17.05s</b>	<b>6.82%</b>	<b>3.68 m/s</b>	<b>93.18%</b>	<b>6.39m/s</b>	<b>25</b>	<b>4.64</b>	<b>7.04ms</b>	<b>1.49</b>	<b>1.39m/s<sup>2</sup></b>

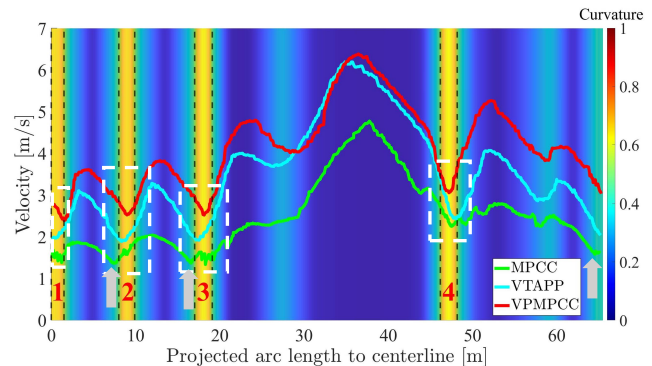
1 The performance of trajectories [11] with globally minimal curvature, based on ideal vehicle handling capabilities, is regarded as vehicle limits.

2 Calculated as  $\frac{T_{lap} - T_{limits}}{T_{lap}}$ . This metric indicates how close the lap time is to reaching the limits. The performance of MPCC is limited by corner '4'.

3 Calculated as  $\frac{\text{Mean}(v_{lap})}{\text{Mean}(v_{limits})}$ . VPMPPC pushes vehicles to limits through the trade-off between velocity prediction and projected velocity maximization.



(a) Racing trajectories correspond to three different methods.



(b) Longitudinal velocities correspond to racing trajectories.

Fig. 6. A schematic of trajectories and vehicle velocities during a single racing lap. The racing trajectory diagram reveals that the locally optimal cornering trajectory differs from the reference line associated with the RVP, as offline trajectory planning cannot account for the real-time states of the vehicle. Furthermore, the velocity diagram shows that VPMPPC achieves the highest cornering velocities, benefiting from its balance between RVP-based velocity prediction and projected velocity maximization in planning optimal local trajectories.

aggressive racing strategy, but the tracking error  $e_s$  is not sufficient to enable it to decelerate in time in corner '4', resulting in a possible collision. As a result, the high-velocity racing parameters of MPCC are restricted in BO training, leaving only parameters with limited racing effects. However, VPMPPC can successfully plan optimal local trajectories in corners by incorporating velocity prediction. This reduces cornering time while ensuring collision-free maneuvers, allowing VPMPPC to achieve higher global racing velocities and ultimately reduce lap time. This is also proved by optimal costs of MPCC and VPMPPC in Fig. 7, while MPCC successfully passes corner '4', its parameters cause a premature deceleration in corners '1' to '3' (pointed out by  $\uparrow$  in Fig. 6b), leading to a loss in racing performance. In contrast, VPMPPC achieves an optimal velocity profile at each sharp corner. Additionally, the cost changes of VPMPPC are smoother compared to MPCC, which further enhances the efficiency of solving the optimization problem (as shown in Fig. 5c).

## VI. CONCLUSIONS

This paper proposes a novel data-driven framework for aggressive autonomous racing that pushes the vehicle to its handling limits. By integrating velocity prediction into local trajectory planning, the vehicle's mean velocity reaches **93.18%** of its handling limits. The training efficiency of

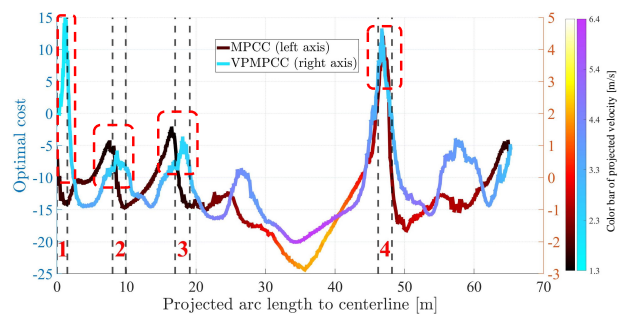


Fig. 7. Demonstration of the cost for MPCC and VPMPPC in real vehicle racing. High costs indicate lower velocities. MPCC cannot plan optimal velocity profiles at corners, leading to premature deceleration at corners '1' to '3'. In contrast, VPMPPC utilizes velocity prediction to balance projected velocity maximization, maintaining optimal velocities at each corner, thus maximizing racing performance.

BO is improved by **42.86%** through the proposed objective function adapted to racing. By filtering out unqualified racing trajectories during BO training, the parameters trained in simulation can be directly transferred to a real-world vehicle without retraining. Future work will explore applying VPMPPC to complex multi-vehicle racing scenarios and integrating deep reinforcement learning for decision-making.

## REFERENCES

- [1] F. Christ, A. Wischniewski, A. Heilmeyer, and B. Lohmann, "Time-optimal trajectory planning for a race car considering variable tyre-road friction coefficients," *Vehicle System Dynamics*, vol. 59, no. 4, pp. 588–612, Apr. 2021.
- [2] C. Hu, L. Xie, Z. Zhang, and H. Xiong, "A novel model predictive controller for the drifting vehicle to track a circular trajectory," *Vehicle System Dynamics*, pp. 1–30, May 2024.
- [3] C. Hu, X. Zhou, R. Duo, H. Xiong, Y. Qi, Z. Zhang, and L. Xie, "Combined Fast Control of Drifting State and Trajectory Tracking for Autonomous Vehicles Based on MPC Controller," in *2022 International Conference on Robotics and Automation (ICRA)*. IEEE, May 2022, pp. 1373–1379.
- [4] W. Xu, Q. Wang, and J. M. Dolan, "Autonomous Vehicle Motion Planning via Recurrent Spline Optimization," in *2021 IEEE International Conference on Robotics and Automation (ICRA)*, May 2021, pp. 7730–7736.
- [5] H. Fan, F. Zhu, C. Liu, L. Zhang, L. Zhuang, D. Li, W. Zhu, J. Hu, H. Li, and Q. Kong, "Baidu apollo em motion planner," 2018.
- [6] J. Schulman, Y. Duan, J. Ho, A. Lee, I. Awwal, H. Bradlow, J. Pan, S. Patil, K. Goldberg, and P. Abbeel, "Motion planning with sequential convex optimization and convex collision checking," *The International Journal of Robotics Research*, vol. 33, no. 9, pp. 1251–1270, Aug. 2014.
- [7] Z. Han, Y. Wu, T. Li, L. Zhang, L. Pei, L. Xu, C. Li, C. Ma, C. Xu, S. Shen, and F. Gao, "An Efficient Spatial-Temporal Trajectory Planner for Autonomous Vehicles in Unstructured Environments," *IEEE Transactions on Intelligent Transportation Systems*, vol. 25, no. 2, pp. 1797–1814, Feb. 2024.
- [8] L. P. Fröhlich, C. Küttel, E. Arcari, L. Hewing, M. N. Zeilinger, and A. Carron, "Contextual Tuning of Model Predictive Control for Autonomous Racing," in *2022 IEEE/RSJ International Conference on Intelligent Robots and Systems (IROS)*. IEEE, Oct. 2022, pp. 10 555–10 562.
- [9] M. Krinner, A. Romero, L. Bauersfeld, M. Zeilinger, A. Carron, and D. Scaramuzza, "Time-optimal flight with safety constraints and data-driven dynamics," *arXiv preprint arXiv:2403.17551*, 2024.
- [10] B. Zhou, C. Hu, Y. Shi, X. Hu, L. Xie, and H. Su, "Learning-based hierarchical model predictive control for drift vehicles," in *2024 American Control Conference (ACC)*, 2024, pp. 3524–3530.
- [11] L. H. J. B. M. L. Alexander Heilmeyer, Alexander Wischniewski and B. Lohmann, "Minimum curvature trajectory planning and control for an autonomous race car," *Vehicle System Dynamics*, vol. 58, no. 10, pp. 1497–1527, 2020. [Online]. Available: <https://doi.org/10.1080/00423114.2019.1631455>
- [12] L. Lyons and L. Ferranti, "Curvature-Aware Model Predictive Contouring Control," in *2023 IEEE International Conference on Robotics and Automation (ICRA)*. IEEE, May 2023, pp. 3204–3210.
- [13] A. Liniger, A. Domahidi, and M. Morari, "Optimization-based autonomous racing of 1:43 scale RC cars," *Optimal Control Applications and Methods*, vol. 36, no. 5, pp. 628–647, Sep. 2015.
- [14] J. Kabzan, M. I. Valls, V. J. F. Reijgwart, H. F. C. Hendrikx, C. Ehmke, M. Prajapat, A. Bühler, N. Gosala, M. Gupta, R. Sivanesan, A. Dhall, E. Chisari, N. Karnchanachari, S. Brits, M. Dangel, I. Sa, R. Dubé, A. Gawel, M. Pfeiffer, A. Liniger, J. Lygeros, and R. Siegwart, "AMZ Driverless: The full autonomous racing system," *Journal of Field Robotics*, vol. 37, no. 7, pp. 1267–1294, Oct. 2020.
- [15] J. Kabzan, L. Hewing, A. Liniger, and M. N. Zeilinger, "Learning-based model predictive control for autonomous racing," *IEEE Robotics and Automation Letters*, vol. 4, no. 4, pp. 3363–3370, 2019.
- [16] J. Betz, H. Zheng, A. Liniger, U. Rosolia, P. Karle, M. Behl, V. Krovi, and R. Mangharam, "Autonomous Vehicles on the Edge: A Survey on Autonomous Vehicle Racing," *IEEE Open Journal of Intelligent Transportation Systems*, vol. 3, pp. 458–488, 2022.
- [17] A. Romero, S. Govil, G. Yilmaz, Y. Song, and D. Scaramuzza, "Weighted Maximum Likelihood for Controller Tuning," in *2023 IEEE International Conference on Robotics and Automation (ICRA)*. IEEE, May 2023, pp. 1334–1341.
- [18] F. Berkenkamp, A. Krause, and A. P. Schoellig, "Bayesian optimization with safety constraints: Safe and automatic parameter tuning in robotics," *Machine Learning*, vol. 112, no. 10, pp. 3713–3747, Oct. 2023.
- [19] B. Shahriari, K. Swersky, Z. Wang, R. P. Adams, and N. De Freitas, "Taking the Human Out of the Loop: A Review of Bayesian Optimization," *Proceedings of the IEEE*, vol. 104, no. 1, pp. 148–175, Jan. 2016.
- [20] W. Weng, C. Hu, Z. Li, H. Su, and L. Xie, "An aggressive cornering framework for autonomous vehicles combining trajectory planning and drift control," in *2024 IEEE Intelligent Vehicles Symposium (IV)*. IEEE, Jun. 2024, pp. 2749–2755.
- [21] J. Becker, N. Imholz, L. Schwarzenbach, E. Ghignone, N. Baumann, and M. Magno, "Model- and Acceleration-based Pursuit Controller for High-Performance Autonomous Racing," in *2023 IEEE International Conference on Robotics and Automation (ICRA)*, May 2023, pp. 5276–5283.
- [22] B. Zhou, H. Cheng, Y. Shi, H. Xiaorong, L. Xie, and S. Hongye, "Learning-based hierarchical model predictive control for drift vehicles," in *2024 American Control Conference (ACC)*. IEEE, 2024, pp. 3524–3530.
- [23] W. Hess, D. Kohler, H. Rapp, and D. Andor, "Real-time loop closure in 2d lidar slam," in *2016 IEEE international conference on robotics and automation (ICRA)*. IEEE, 2016, pp. 1271–1278.
- [24] J. A. E. Andersson, J. Gillis, G. Horn, J. B. Rawlings, and M. Diehl, "CasADi – A software framework for nonlinear optimization and optimal control," *Mathematical Programming Computation*, vol. 11, no. 1, pp. 1–36, 2019.